

RSC Advances



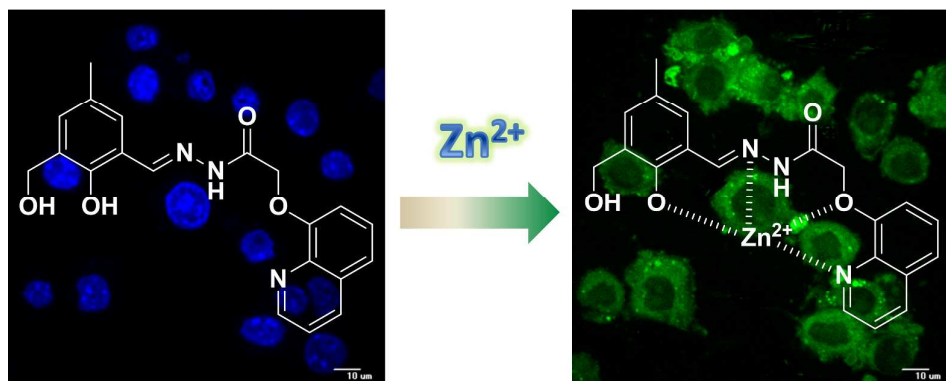
This is an *Accepted Manuscript*, which has been through the Royal Society of Chemistry peer review process and has been accepted for publication.

Accepted Manuscripts are published online shortly after acceptance, before technical editing, formatting and proof reading. Using this free service, authors can make their results available to the community, in citable form, before we publish the edited article. This *Accepted Manuscript* will be replaced by the edited, formatted and paginated article as soon as this is available.

You can find more information about *Accepted Manuscripts* in the [Information for Authors](#).

Please note that technical editing may introduce minor changes to the text and/or graphics, which may alter content. The journal's standard [Terms & Conditions](#) and the [Ethical guidelines](#) still apply. In no event shall the Royal Society of Chemistry be held responsible for any errors or omissions in this *Accepted Manuscript* or any consequences arising from the use of any information it contains.

Graphical Abstract:



ARTICLE

A new ICT and CHEF based visible light excitable fluorescent probe easily detects *in vivo* Zn²⁺

Cite this: DOI: 10.1039/x0xx00000x

Krishnendu Aich,^a Shyamaprosad Goswami,^{*a} Sangita Das^a and Chitragada Das Mukhopadhyay^b

Received 00th January 2012,

Accepted 00th January 2012

DOI: 10.1039/x0xx00000x

www.rsc.org/

A new chelator and ICT donor based visible light excitable Zn²⁺ sensor was designed and developed by integrating quinoline and 2-hydroxy-3-(hydroxymethyl)-5-methylbenzaldehyde. The probe is sensitive towards Zn²⁺ in absorbance as well as in fluorescence experiment in 90% aqueous medium. The sensor demonstrates Zn²⁺-specific emission enhancement due to the ICT and CHEF process with the LOD is in the range of 10⁻⁸ M. The fluorescence quantum yield of chemosensor is only 0.02, and it increases almost 11-fold (0.22) after complexation with Zn²⁺. Interestingly, the introduction of other metal ions causes the fluorescence intensity to remain almost unchanged. Moreover, the ability of the probe (BQ) to sense Zn²⁺ in living cells has been explored.

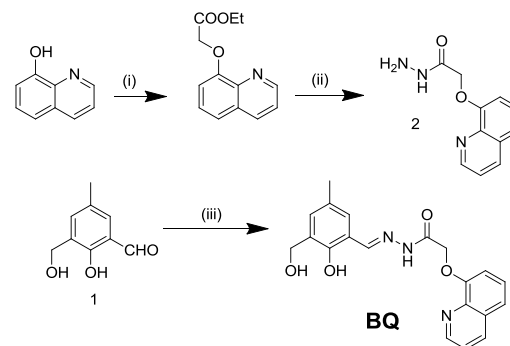
Introduction

Detection and imaging of biologically relevant target molecules through fluorescence in living systems has emerged as an area of intense interest in the chemistry-biology interface owing to its significant biomedical implications.¹ Zn²⁺ has received considerable attention as it is the second most abundant heavy metal ion after iron present in the human body with its total content of 2–3 g in the whole body and its concentration as high as 10 μM in serum.² It is an essential nutrient required for normal growth³ and development. It also play crucial role for the key cellular processes such as DNA repair⁴ and apoptosis.⁵ The deficiency of zinc causes unbalanced metabolism, which in turn can induce retarded growth in children, brain disorders, high blood cholesterol⁶ and also be implicated in various neurodegenerative disorders such as Alzheimer's disease, epilepsy, ischemic stroke, and infantile diarrhea.⁷ Fluorescent Zn²⁺ imaging with Zn²⁺ sensors has demonstrated great success in providing temporal-spatial information of Zn²⁺ homeostasis in live cells.⁸ Therefore, now a days there is a huge demand for the development of Zn²⁺ chemosensors. Fluorescence spectroscopy is a powerful method for sensing and imaging metal cations at submicromolar concentrations.⁹ In recent times, a number of selective and sensitive imaging tools capable of rapidly monitoring Zn²⁺ ions have been developed.¹⁰ Specially development of sensitive sensors which can distinguish the metal ions with almost similar characteristic

(like Zn²⁺/Cd²⁺, Pb²⁺/Hg²⁺ pairs which may interfere in each other detection) are in high demand.

In the context of the above objectives and in continuation of our work,¹¹ in here, we have synthesized a highly sensitive and selective hydroxyquinoline based new visual and fluorescent probe BQ for Zn²⁺. We have screened its potential applications in cell imaging and studied its cytotoxic properties. Interestingly here, Cd²⁺ is found to perturb the fluorescence a slight but the output is different from Zn²⁺.

Results and discussion



Scheme 1: Reagents and conditions: (i) ethylchloroacetate, K₂CO₃, dry acetone, reflux, 12 h. (ii) NH₂NH₂, EtOH, reflux, 2 h, (iii) 2, EtOH, reflux, 6h

Synthesis of BQ is accomplished by reaction of the compounds 2 and 1 in ethanol under refluxing condition for 6h. Compounds 1 and 2 were prepared from according to previously reported procedure.¹² The yield of the final imine functionalized compound obtained to be 65%. The probe (BQ) was characterized by NMR and HRMS studies (Fig. S9-S11, ESI).

Sensing Studies

In order to investigate the metal-binding behavior of the probe (BQ) towards different cations, we have monitored both the UV-visible absorption and fluorescence study of BQ with different cations (Na^+ , K^+ , Mg^{2+} , Cu^{2+} , Mn^{2+} , Fe^{2+} , Fe^{3+} , Co^{2+} , Ni^{2+} , Cd^{2+} , Ca^{2+} , Zn^{2+} and Hg^{2+} as their chloride salts). All of the titration studies of BQ were carried out in $\text{CH}_3\text{OH}/\text{H}_2\text{O}$ (1/9, v/v, 1 mM HEPES buffer at pH = 7.4) solution. The electronic absorption spectral behavior of BQ (10 μM) exhibited two sharp bands at 360 and 282 nm (Figure 1a). Upon gradual addition of aqueous solution of Zn^{2+} (0-1.5 equiv.), the bands at 360 and 282 nm gradually decreased along with a new peak appeared at 405 nm, which readily increased with Zn^{2+} concentration. This new peak is being attributed to internal charge transfer (ICT) of BQ after interaction with Zn^{2+} . This spectral behavior consecutively showed three well-defined isosbestic points centred at 380 nm, 340 nm and 305 nm.

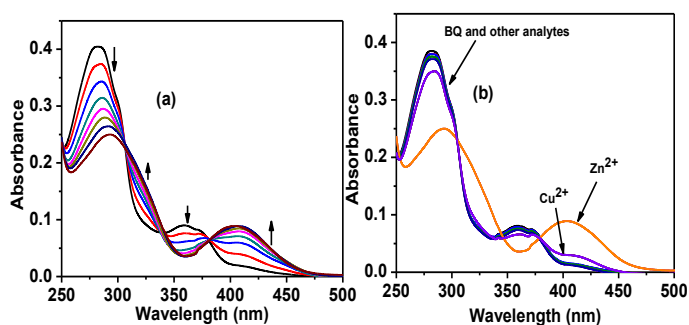


Figure 1: UV-vis spectra of BQ (10 μM) in $\text{CH}_3\text{OH}/\text{H}_2\text{O}$ solution (1/9, v/v, pH = 7.4) in presence of (a) Zn^{2+} (0-1.5 equivalents) and (b) different analytes (3 equivalents).

Furthermore, BQ exhibits a good linear relationship of absorbance ratio (A_{405}/A_{282}) with added Zn^{2+} concentration (0 to 9 μM , Fig S2, ESI). The strong binding of Zn^{2+} with BQ was further supported by the association constant determined from Benesi-Hildebrand plot¹³ by using UV-vis data and it was found to be $5.77 \times 10^5 \text{ M}^{-1}$ (Fig. S4, ESI). Notably, the addition of other metal cations did not perturb the initial absorption spectrum of the chemosensor significantly (except Cu^{2+} , in here a slight change was noticed). From these UV-vis spectral studies, it is obvious that the probe BQ revealed a very high affinity towards Zn^{2+} in the ground state.

The fluorescence spectrum of the probe BQ (10 μM) exhibited a weak emission band centered at 435 nm in $\text{CH}_3\text{OH}/\text{H}_2\text{O}$ solution (1/9, v/v, 1 mM HEPES buffer at pH = 7.4) upon excitation at 400 nm. On incremental addition of Zn^{2+} (0-1.5 equiv.) to the solution of the probe BQ, the fluorescence

emission exhibited an enhancement along with a red shift from 435 nm to 475 nm. This dramatic red shift (~ 40 nm) of the fluorescence of BQ after introduction of Zn^{2+} was attributed to the internal charge transfer (ICT). In addition, the emission band at 475 nm significantly enhanced after incremental addition of Zn^{2+} (Figure 2a). During the course of titration the intensity at 475 nm (I_{475}) exhibited a beautiful linear relationship with Zn^{2+} concentration (0 to 9 μM , Fig S1b, ESI) with a R^2 value of 0.9807.

This overall spectral behavior of fluorescence enhancement of the probe BQ after being induced by Zn^{2+} may be due to the contribution of two mechanisms, namely ICT and CHEF mechanism. BPQ itself exhibited a weak fluorescence intensity at 435 nm, which may be due to the occurrence of $-E$, $-Z$ isomerism for free rotation of the imine ($-\text{C}=\text{N}$) segment.

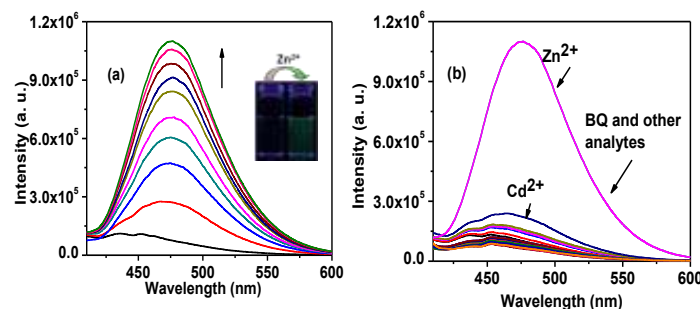
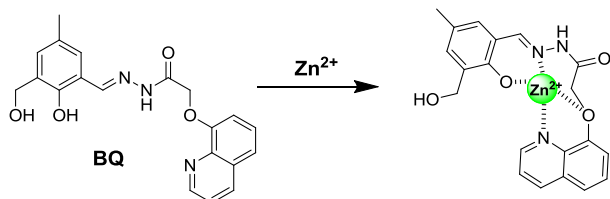


Figure 2: Emission spectra of BQ (10 μM) in ($\text{MeOH}/\text{H}_2\text{O}$, 1/9, v/v, pH = 7.4) in presence of (a) Zn^{2+} (0-1.5 equivalents) and (b) different analytes (4 equivalents). Inset: emission colour change of BQ upon addition of 2 equivalents of Zn^{2+} after illumination under UV light. $\lambda_{\text{ex}} = 400$ nm.

Now the introduction of Zn^{2+} , this kind of (E -, Z -) isomerism may stop and CHEF mechanism may come into play, which ultimately formed a stable chelate complex between the cation (Zn^{2+}) and the probe BQ. The addition of Zn^{2+} eventually made the system more rigid (Scheme 2) and revealed a fabulous increment in emission profile. The formation of 1:1 complexation with Zn^{2+} was confirmed by Job's plot (Figure S6) and HRMS data, it shows peaks at m/z 451.0923, which may be due to the formation of BQ- Zn^{2+} complex species.

Now selectivity and specificity are the two very important factors in order to evaluate the efficiency of any probe. So to prove the selectivity of the probe BQ toward Zn^{2+} ions, we carried out the fluorescence titration experiment of BQ in presence of other above mentioned cations. It was found that the probe was prone to Zn^{2+} only (selective enhancement of emission at 475 nm) and this affinity was very much prominent even in the presence of other guest metal ions (Figure S7, ESI). Thus all these experiments established that the probe BQ showed a major response only towards Zn^{2+} and it can detect exclusively Zn^{2+} at 475 nm without any noticeable interference. In the fluorescence titration experiment of BQ, a different interference was noticed with Cd^{2+} , it showed a slight change in emission at 465 nm but no interference at 475 nm. From this fluorescence experiment it was demonstrated that, the probe BQ was capable to detect back to back two of very similar

cations with two different outputs (for Zn^{2+} it is a strong peak at 475 nm and for Cd^{2+} a weak peak at 465 nm). To determine the limit of detection i.e how lower concentration of Zn^{2+} can be determined by the probe (BQ), we recorded the fluorescence data using 10 μM solution (CH_3OH/H_2O , 1/9, v/v, 1mM HEPES buffer, pH =7.4) of BQ (Fig S1b, ESI). The detection limit of BQ for Zn^{2+} was determined to be 2.35×10^{-8} M, using the equation $DL = K \times Sb_1/S$, where $K = 3$, Sb_1 is the standard deviation of the blank solution and S is the slope of the calibration curve¹⁴ (Figure S1, ESI).



Scheme 2: Probable binding mode of BQ with Zn^{2+}

pH study

In order to examine the pH sensitivity of our probe BQ, we examined the acid–base titration experiment. From the titration study it was observed that BQ does not undergo any noticeable change in the fluorescence profile within the pH range from 2–8. But in strong basic conditions (pH > 9), deprotonation of the phenolic group causes the coloration along with strong green fluorescence (Fig. S8a, ESI). Thus BQ can be employed for the detection of Zn^{2+} in near-neutral pH range (pH = 7.4). The pH sensitivity of BQ in presence of Zn^{2+} was also studied. The results revealed that in strong acidic pH (< 3) and in strong basic pH (> 10) detection of Zn^{2+} was a little bit hampered. But in the pH range of 3 to 9, BQ can detect Zn^{2+} with no such interference (Fig. S8b, ESI).

Live-cell imaging study

Cell viability assay

Considerations of the practical application of thermodynamic favourable binding properties of BQ with Zn^{2+} led to the further examination of the ability of the probe (BQ) to sense Zn^{2+} in the living cells. In order to fulfil this objective it is important to determine the cytotoxic effect of BQ and Zn^{2+} and the complex on live cells. The well-established MTT assay, which is based on mitochondrial dehydrogenase activity of viable cells, was adopted to study cytotoxicity of above mentioned compounds at varying concentrations mentioned in method section. Figure 3 shows that probe compound did not exert any adverse effect on cell viability; same is the case when cells were treated with varying concentrations of $ZnCl_2$. However, exposure of HCT cells to probe– Zn^{2+} complex resulted in a decline in cell viability above 20 μM concentration.

The effect was more pronounced in higher concentration and showed an adverse cytotoxic effect in a dose-dependent manner. The viability of HCT cells was not influenced by the

solvent (DMSO) as evidenced in Figure 3, leading to the conclusion that the observed cytotoxic effect could be attributed to probe– Zn^{2+} complex. The results obtained in the in vitro cytotoxic assay suggested that, in order to pursue fluorescence imaging studies of probe– Zn^{2+} complex in live cells, it would be prudent to choose a working concentration of 10 μM for probe compound.

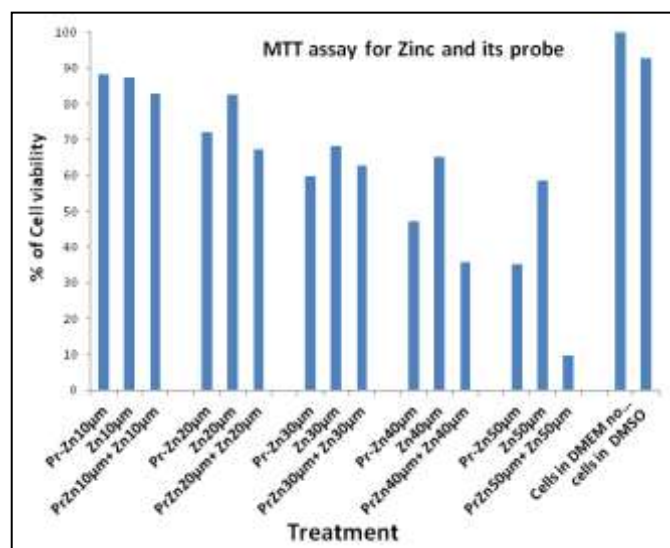


Figure 3: It represents % cell viability of HCT cells treated with different concentrations (10 μM –50 μM) of BQ for 12 hrs determined by MTT assay. Results are expressed as mean of three independent experiments.

Imaging of cells

Fluorescence microscopic studies revealed a lack of fluorescence for RAW cells when treated with either probe compound (10 μM) or $ZnCl_2$ (20 μM) alone (Figure 4, panel a & b).

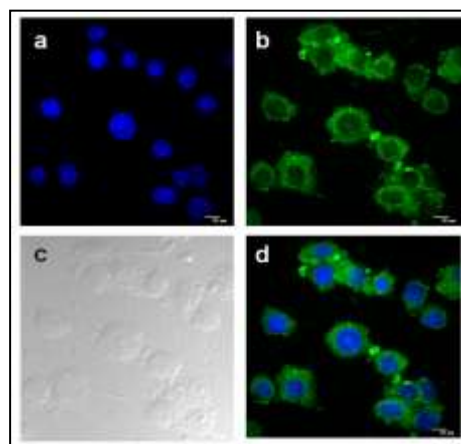


Figure 4: Confocal microscopic images of probe in RAW 264.7 cells pretreated with $ZnCl_2$: (a) $ZnCl_2$ treatment only at 2.0×10^{-5} M concentration, nuclei counterstained with DAPI (1 $\mu g/ml$), (b) treatment a followed by probe BQ at concentration 1.0×10^{-5} M, (c) bright field image of the cells after treatment (d)

overlay image in dark field. All images were acquired with a 60× objective lens with a scale bar of 10 μm. λ_{ex} = 400 nm.

Upon incubation with ZnCl₂ followed by probe compound a striking green fluorescence was observed inside RAW cells, which indicated the formation of Probe- Zn²⁺ complex, as observed earlier in solution studies. Further, an intense green fluorescence was conspicuous in the perinuclear region of RAW cells (Figure 4, panel b) which indicates that the probe can penetrate cell membrane easily and can be used to detect Zn²⁺ in cells. The fluorescence microscopic analysis strongly suggested that probe could readily cross the membrane barrier, permeate into RAW cells, and rapidly sense intracellular Zn²⁺. It is significant to mention here that bright field images of treated cells did not reveal any gross morphological changes, which suggested that RAW cells were viable. These findings open up the avenue for future *in vivo* biomedical applications of the probe to image intracellular Zn²⁺.

Experimental

General

Unless otherwise mentioned, materials were obtained from commercial suppliers and were used without further purification. Thin layer chromatography (TLC) was carried out using Merck 60 F₂₅₄ plates with a thickness of 0.25 mm. Melting points were determined on a hot-plate melting point apparatus in an open-mouth capillary and are uncorrected. ¹H and ¹³C NMR spectra were recorded on JEOL 400 MHz and 125 MHz instruments respectively. For NMR spectra, CDCl₃ and d⁶-DMSO were used as solvents using TMS as an internal standard. Chemical shifts are expressed in δ units and ¹H-¹H and ¹H-C coupling constants in Hz. UV-vis spectra were recorded on a JASCO V-630 spectrometer. Fluorescence spectra were recorded on a Perkin Elmer LS 55 fluorescence spectrometer. IR spectra were recorded on a JASCO FT/IR-460 plus spectrometer, using KBr discs. For the titration experiment, we use the cations viz. [Na⁺, K⁺, Mg²⁺, Cu²⁺, Mn²⁺, Fe²⁺, Fe³⁺, Co²⁺, Ni²⁺, Ca²⁺, Cd²⁺, Zn²⁺ and Hg²⁺ as their chloride salts.

General method of UV-vis and fluorescence titration

UV-vis method

For UV-vis titrations, stock solution of the receptor (10 μM) was prepared in [(CH₃OH / water), 1/9, v/v] (at 25°C) using 1 mM HEPES buffered pH 7.4 solution. The solutions of the guest cations using their chloride salts in the order of 1 × 10⁻⁵ M, were prepared in deionized water using HEPES buffer at pH = 7.4. Solutions of various concentrations containing the sensor and increasing concentrations of cations were prepared separately. The spectra of these solutions were recorded by means of UV-vis method.

Fluorescence method

For fluorescence titrations, stock solution of the sensor (10 μM) used was the same as that used for UV-vis titration. The solutions of the guest cations using their chloride salts in the order of 1 × 10⁻⁵ M, were prepared same as stated in UV-vis experiment. Solutions of various concentrations containing sensor and increasing concentrations of cations were prepared separately. The spectra of these solutions were recorded by means of fluorescence method.

Determination of fluorescence quantum yield

To determine the quantum yields of BQ and BQ-Zn²⁺, we recorded their absorbance in methanol solution. The emission spectra were recorded using the maximal excitation wavelengths, and the integrated areas of the fluorescence-corrected spectra were measured. The quantum yields were then calculated by comparison with fluorescein ($\Phi_s = 0.97$ in basic ethanol) as reference using the following equation:

$$\Phi_x = \Phi_s \times (I_x/I_s) \times (A_s/A_x) \times (n_x/n_s)^2$$

Where, x & s indicate the unknown and standard solutions respectively, Φ is the quantum yield, I is the integrated area under the fluorescence spectra, A is the absorbance and n is the refractive index of the solvent.

Synthetic method for the preparation of the probe

To the stirred solution of compound 2 (0.25 g, 1.15 mmol) in ethanol, 2-hydroxy-3-(hydroxymethyl)-5-methylbenzaldehyde (0.2 g, 1.20 mmol) was added and the reaction mixture was refluxed for 6 hours. After ensuring that the reactants were fully consumed, by checking TLC, the reaction mixture was allowed to cool to room temperature. A white precipitate appeared which was filtered, washed with cold ethanol (1ml × 2) and dried in air. Yield = (0.27 g) 65%.

¹H NMR (400 MHz, d₆-DMSO): δ 2.24 (s, 3H), 4.52 (s, 2H), 4.59 (s, 2H), 7.14 (s, 1H), 7.21 (t, J = 7.8 Hz, 1H), 7.30 (d, J = 8Hz, 1H), 7.56 (m, 3H), 8.38 (dd, 1H), 8.46 (s, 1H), 8.96 (dd, 1H), 11.44 (s, 1H), 12.33 (s, 1H).

¹³C NMR (125 MHz, d₆-DMSO): δ 20.0, 57.5, 68.7, 112.9, 116.6, 121.3, 122.0, 127.2, 127.5, 128.9, 129.2, 129.4, 130.1, 131.9, 135.4, 148.5, 150.2, 152.4, 152.8, 164.0

HRMS (ESI, positive): calcd. for C₂₀H₁₉N₃NaO₄ [M + Na]⁺ (m/z): 388.1273; found: 388.1275.

Synthesis of Zn²⁺ complex (BQ-Zn²⁺) of receptor

The receptor, BQ (40 mg) and ZnCl₂ (10 mg) were mixed together and dissolved in 5 ml of methanol. After reflux for 12 hours the reaction mixture was cooled to room temperature. A reddish-yellow coloured precipitate appeared which was filtered and dried in vacuum.

HRMS (ESI, Positive): calcd. for C₂₀H₁₈ZnN₃NaO₄ [M + Zn²⁺ + Na⁺ + H⁺]⁺ (m/z): 451.0476; found: 451.0923.

Details of live-cell imaging

Materials Methods

Frozen Human colorectal carcinoma cell lines **HCT 116 (ATCC : CCL-247)** were obtained from the American Type Culture Collection (Rockville, MD, USA) and maintained in Dulbecco's modified Eagle's medium (DMEM, Sigma Chemical Co., St. Louis, MO, USA) supplemented with 10% fetal bovine serum (Invitrogen), penicillin (100 µg/ml), and streptomycin (100 µg/ml). The RAW 264.7 macrophages were obtained from NCCS, Pune, India and maintained in DMEM containing 10% (v/v) fetal calf serum and antibiotics in a CO₂ incubator. Cells were initially propagated in 25 cm² tissue culture flask in an atmosphere of 5% CO₂ and 95% air at 37°C humidified air till 70- 80% confluency.

Fluorescent imaging studies

For fluorescent imaging studies, RAW cells, 7.5×10³ cells in 150 µl media were seeded on sterile 12 mm diameter Poly L lysine coated cover-slip and kept in a sterile 35mm covered Petri dish and incubated at 37°C in a CO₂ incubator for 24-30 h. Next day cells were washed three times with phosphate buffered saline (pH 7.4) and fixed using 4% paraformaldehyde in PBS (pH 7.4) for 10 minutes at room temperature washed with PBS followed by permeabilization using 0.1% saponin for 10 minutes. Then the cells were incubated with 2.0 × 10⁻⁵ M ZnCl₂ dissolved in 100 µl DMEM at 37 °C for 1 h in a CO₂ incubator and observed under 60X magnification of Andor spinning disc confocal microscope. The cells were again washed thrice with PBS (pH 7.4) to remove any free metal and incubated in DMEM containing probe (BQ) to a final concentration of 1.0 × 10⁻⁵ M followed by washing with PBS (pH 7.4) three times to remove excess probe outside the cells. Again, images were acquired. Before fluorescent imaging all the solutions were aspirated out and cover slips containing cells were mounted on slides in a mounting medium containing DAPI, (4',6-Diamidino-2-Phenylindole) in 1µg/ml concentration. DAPI is a popular nuclear counterstain used in multicolor fluorescent imaging of cells. It preferentially stains dsDNA and its blue fluorescence stands out in contrast to green, yellow, or red fluorescent probes of other structures with little or no cytoplasmic labelling. Finally the slides were stored in dark before microscopic images are acquired.

Cytotoxicity assay

The cytotoxic effects of probe, ZnCl₂ and probe-ZnCl₂ complex were determined by an MTT assay following the manufacturer's instruction (MTT 2003, Sigma-Aldrich, MO). HCT cells were cultured into 96-well plates (approximately 10⁴ cells per well) for 24 h. Next day media was removed and various concentrations of probe, ZnCl₂ and probe-ZnCl₂ complex (0, 15, 25, 50, 75, and 100 µM) made in DMEM were added to the cells and incubated for 24 h. Solvent control samples (cells treated with DMSO in DMEM), no cells and cells in DMEM without any treatment were also included in the study. Following incubation, the growth media were removed, and fresh DMEM containing MTT solution was added. The plate was incubated for 3-4 h at 37°C. Subsequently, the supernatant was removed, the insoluble colored formazan product was solubilized in DMSO, and its absorbance was measured in a microtiter plate reader (Perkin-Elmer) at 570 nm.

The assay was performed in triplicate for each concentration of probe, ZnCl₂ and probe-CdCl₂ complex. The OD value of wells containing only DMEM medium was subtracted from all readings to get rid of the background influence. Data analysis and calculation of standard deviation were performed with Microsoft Excel 2007 (Microsoft Corporation).

Conclusions

In summary, a new quinoline based probe BQ was synthesized, which is an excellent fluorescent sensor for detection of Zn²⁺. This phenomenon was observed due to the ICT-CHEF mechanism only after introduction of Zn²⁺ in BQ solution. Zn²⁺ exhibits a tremendous increment in fluorescence intensity at 475 nm only after introduction of Zn²⁺ in BQ solution. The photophysical study shows that the probe forms 1:1 complex with Zn²⁺. It produces a remarkably high selectivity toward Zn²⁺ ion over other competitive cations, such as Na⁺, K⁺, Mg²⁺, Cu²⁺, Mn²⁺, Fe²⁺, Fe³⁺, Co²⁺, Ni²⁺ and Hg²⁺. The twist is in the fluorescence spectra with Cd²⁺ which shows fluorescence intensity at 465 nm. Most importantly, a discrimination of two metal ions (Zn²⁺ and Cd²⁺) of almost similar characteristic can be achieved by the probe in hand. The detection limit was found to be in 10⁻⁸ M range. Moreover the probe BQ could be a suitable platform for Zn²⁺ imaging in biological system.

Acknowledgements

Authors thank the CSIR and DST, Govt. of India for financial supports. K.A and S.D acknowledge CSIR for providing them fellowships.

Notes and references

^a Department of Chemistry, Indian Institute of Engineering Science and Technology, Shibpur, Howrah-711 103, India.

E-mail: spgoswamical@yahoo.com

^bCentre for Healthcare Science & Technology, Indian Institute of Engineering Science and Technology, Shibpur, Howrah-711 103, India.

†Electronic Supplementary Information (ESI) available: [details of any supplementary information available should be included here]. See DOI: 10.1039/b000000x/

1. (a) P. N. Prasad, *Introduction to Biophotonics*, Wiley, NJ, 2003; (b) J. W. Lichtman and J.-A. Conchello, *Nat. Methods*, 2005, **2**, 910.
2. (a) J. M. Berg and Y. Shi, *Science*, 1996, **271**, 1081; (b) M. Lu and D. Fu, *Science*, 2007, **317**, 1746.
3. (a) C. J. Frederickson, J.-Y. Koh and A. I. Bush, *Nat. Rev. Neurosci.*, 2005, **6**, 449; (b) M. Cortesi, R. Chechik, A. Breskin, D. Vartsky, J. Ramon, G. Raviv, A. Volkov and E. Fridman, *Phys. Med. Biol.*, 2009, **54**, 781.
4. (a) E. Ho and B. N. Ames, *Proc. Natl. Acad. Sci. U. S. A.*, 2002, **99**, 16770; (b) H. Daiyasu, K. Osaka, Y. Ishino and H. Toh, *FEBS Lett.*, 2001, **503**, 1.
5. A. Q. Troung-Tran, J. Carter, R. E. Ruffin and P. D. Zalewski, *BioMetals*, 2001, **14**, 315.

6. (a) E. F. Rostan, H. V. DeBuys, D. L. Madey and S. R. Pinnell, *Int. J. Dermatol.*, 2002, **41**, 606; (b) Z. Sztányi, C. Nemes and N. Rozlosnik, *Cent Eur. J. Occup. Environ. Med.*, 1998, **4**, 51.
7. A. I. Bush, W. H. Pettingell, G. Multhaup, M. Paradis, J.-P. Vonsattel, J. F. Gusella, K. Beyreuther, C. L. Masters and R. E. Tanzi, *Science*, 1994, **265**, 1464.
8. (a) E. Tomat and S. J. Lippard, *Curr. Opin. Chem. Biol.*, 2010, **14**, 225; (b) Z. Xu, J. Yoon and D. R. Spring, *Chem. Soc. Rev.*, 2010, **39**, 1996; (c) E. L. Que, D. W. Domaille and C. J. Chang, *Chem. Rev.*, 2008, **108**, 1517; (d) P. Jiang and Z. Guo, *Coord. Chem. Rev.*, 2004, **248**, 205.
9. (a) A. P. de Silva, H. Q. N. Gunaratne, T. Gunnlaugsson, A. J. M. Huxley, C. P. McCoy, J. T. Rademacher, T. E. Rice, *Chem. Rev.* 1997, **97**, 1515; (b) B. Valeur and I. Leray, *Coord. Chem. Rev.*, 2000, **205**, 3; (c) B. Valeur, *Molecular Fluorescence: Principles and Applications*, Wiley-VCH, Weinheim, 2001; (d) G. Sivaraman, T. Anand and D. Chellappa, *ChemPlusChem*, 2014, **79**, 1761; (e) T. Anand, G. Sivaraman, A. Mahesh and D. Chellappa, *Analytica Chimica Acta*, 2015, **853**, 596; (f) G. Sivaraman, B. Vidya and D. Chellappa, *RSC Adv.*, 2014, **4**, 30828; (g) L. E. Santos-Figueroa, M. E. Moragues, E. Climent, A. Agostini, R. Martínez-Mañez and F. Sancenón, *Chem. Soc. Rev.*, 2013, **42**, 3489; (h) S. Lee, K. K. Y. Yuen, K. A. Jolliffe and J. Yoon, *Chem. Soc. Rev.*, 2015, DOI: 10.1039/C4CS00353E; (i) N. A. Esipenko, P. Koutnik, T. Minami, L. Mosca, V. M. Lynch, G. V. Zyryanov and P. Anzenbacher, Jr., *Chem. Sci.*, 2013, **4**, 3617; (j) S. Turkyilmaz, D. R. Rice, R. Palumbo and B. D. Smith, *Org. Biomol. Chem.*, 2014, **12**, 5645.
10. (a) K. R. Gee, Z. L. Zhou, W. J. Qian and R. Kennedy, *J. Am. Chem. Soc.*, 2002, **124**, 776; (b) E. J. Song, J. Kang, G. R. You, G. J. Park, Y. Kim, S.-J. Kim, C. Kim and R. G. Harrison, *Dalton Trans.*, 2013, **42**, 15514; (c) G. K. Tsikalas, P. Lazarou, E. Klontzas, S. A. Pergantis, I. Spanopoulos, P. N. Trikalitis, G. E. Froudakis and H. E. Katerinopoulos, *RSC Adv.*, 2014, **4**, 693; (d) K. B. Kim, H. Kim, E. J. Song, S. Kim, I. Noh and C. Kim, *Dalton Trans.*, 2013, **42**, 16569; (e) P. Li, X. Zhou, R. Huang, L. Yang, X. Tang, W. Dou, Q. Zhao and W. Liu, *Dalton Trans.*, 2014, **43**, 706; (f) Z. Liu, C. Zhang, Y. Chen, F. Qian, Y. Bai, W. He and Z. Guo, *Chem. Commun.*, 2014, **50**, 1253; (g) T.-T. Zhang, X.-P. Chen, J.-T. Liu, L.-Z. Zhang, J.-M. Chu, L. Su and B.-X. Zhao, *RSC Adv.*, 2014, **4**, 16973; (h) V. Bhalla, Roopa and M. Kumar, *Dalton Trans.*, 2013, **42**, 975; (i) Z. Xu, K.-H. Baek, H. N. Kim, J. Cui, X. Qian, D. R. Spring, I. Shin and J. Yoon, *J. Am. Chem. Soc.* 2010, **132**, 601; (j) N. Y. Baek, C. H. Heo, C. S. Lim, G. Masanta, B. R. Cho and H. M. Kim, *Chem. Commun.*, 2012, **48**, 4546; (k) B. K. Datta, D. Thiyagarajan, S. Samanta, A. Ramesh and G. Das, *Org. Biomol. Chem.*, 2014, **12**, 4975; (l) J. Pancholi, D. J. Hodson, K. Jobe, G. A. Rutter, S. M. Goldup and M. Watkinson, *Chem. Sci.*, 2014, **5**, 3528; (m) Z. Dong, X. Le, P. Zhou, C. Dong and J. Ma *New J. Chem.*, 2014, **38**, 1802; (n) P. Li, X. Zhou, R. Huang, L. Yang, X. Tang, W. Dou, Q. Zhao and W. Liu, *Dalton Trans.*, 2014, **43**, 706; (o) Y. Xu, L. Xiao, S. Sun, Z. Pei, Y. Pei and Y. Pang, *Chem. Commun.*, 2014, **50**, 7514; (p) N. Khairnar, K. Tayade, S. K. Sahoo, B. Bondhopadhyay, A. Basu, J. Singh, N. Singh, V. Gite and A. Kuwar, *Dalton Trans.*, 2015, **44**, 2097; (q) G. Sivaraman, T. Anand and D. Chellappa, *Analyst*, 2012, **137**, 5881; (r) P. Kaleeswaran, I. A. Azath, V. Tharmaraj and K. Pitchumani, *Chem plus chem*, 2014, **79**, 1361; (s) G. Sivaraman, T. Anand and D. Chellappa, *Anal. Methods*, 2014, **6**, 2343; (t) E. M. Nolan, S. J. Lippard, *Acc Chem Res.*, 2009, **42**, 193; (u) H. T. Ngo, X. Liu and K. A. Jolliffe, *Chem. Soc. Rev.*, 2012, **41**, 4928.
11. (a) S. Goswami, S. Das, K. Aich, D. Sarkar and T. K. Mondal, *Tetrahedron Lett.* 2013, **54**, 6892; (b) S. Goswami, S. Das, K. Aich, D. Sarkar and T. K. Mondal, *Tetrahedron Lett.*, 2014, **55**, 2695; (c) S. Goswami, K. Aich, S. Das, S. B. Roy, B. Pakhira and S. Sarkar, *RSC Advances*, 2014, **4**, 14210; (d) S. Goswami, K. Aich, S. Das, A. K. Das, A. Manna, S. Halder, *Analyst*, 2013, **138**, 1903; (e) S. Goswami, K. Aich, D. Sen, *Chem. Lett.* 2012, **41**, 863; (f) S. Goswami, S. Das, K. Aich, D. Sarkar, T. K. Mondal, C. K. Quah and H.-K. Fun, *Dalton Trans.*, 2013, **42**, 15113; (g) S. Goswami, S. Das, K. Aich, B. Pakhira, S. Panja, S. K. Mukherjee and S. Sarkar, *Org. Lett.*, 2013, **15**, 5412; (h) S. Goswami, S. Das and K. Aich, *Tetrahedron Lett.*, 2013, **54**, 4620; (i) S. Goswami, K. Aich, S. Das, A. K. Das, D. Sarkar, S. Panja, T. K. Mondal and S. K. Mukhopadhyay, *Chem. Commun.*, 2013, **49**, 10739; (j) S. Goswami, K. Aich, S. Das, B. Pakhira, K. Ghoshal, C. K. Quah, M. Bhattacharyya, H.-K. Fun and S. Sarkar, *Chem. Asian J.*, 2015, **10**, 694; (k) S. Goswami, K. Aich, S. Das, C. D. Mukhopadhyay, D. Sarkar and T. K. Mondal, *Dalton Trans.*, 2015, **44**, 5763.
12. S. Goswami, K. Aich, A. K. Das, A. Manna and S. Das, *RSC Adv.*, 2013, **3**, 2412.
13. (a) H. A. Benesi and J. H. Hildebrand, *J. Am. Chem. Soc.*, 1949, **71**, 2703; (b) D. C. Carter and J. X. Ho, *Adv. Protein Chem.*, 1994, **45**, 153; (c) A. Mallick and N. Chattopadhyay, *Photochem. Photobiol.*, 2005, **81**, 419; (d) I. Ravikumar, B. N. Ahamed and P. Ghosh, *Tetrahedron*, 2007, **63**, 12940.
14. (a) M. Shortreed, R. Kopelman, M. Kuhn and B. Hoyland, *Anal. Chem.*, 1996, **68**, 1414; (b) W. Lin, L. Yuan, Z. Cao, Y. Feng and L. Long, *Chem.–Eur. J.*, 2009, **15**, 5096.